JMEPEG (2012) 21:1873–1878
DOI: 10.1007/s11665-011-0089-8

1059-9495/$19.00

Effect of the Spinning Deformation Processing on Mechanical Properties of Al-7Si-0.3Mg Alloys

Yin-Chun Cheng, Chih-Kuang Lin, An-Hung Tan, Shih-Yuan Hsu, and Sheng-Long Lee

(Submitted April 12, 2011; in revised form November 10, 2011)

This study investigates the mechanical properties of Al-7Si-0.3Mg (A356) alloy affected by the spinning deformation processing (SDP). The cast structure of the A356 alloy becomes elongated with increasing reduction in thickness. This leads to reduction of casting defects, and refines and distributes the eutectic silicon phase throughout the Al-matrix. The hardness tends to reach a steady value due to the uniformity of the microstructure with the reduction in thickness. The SDP leads to a re-arrangement in the eutectic region, which forces the propagation of cracks through the ductile α-Al phase. The tensile strength and elongation increases accordingly. The improvement on tensile strength and elongation produces the best quality index for A356 alloy.

Keywords aluminum, elongation, spinning

1. Introduction

The demand for fuel efficiency in transportation has been growing in recent years, which has encouraged the development of light-weight components, optimal designs, better choice of materials, and suitable manufacturing processes. For example, light automobile wheels made of aluminum alloys can improve ride and handling and fuel consumption of the vehicle, so are generally adopted by automakers (Ref 1). Cast aluminum wheels have the advantages of cheap price and flexible styling, so have become a mainstream product in the market. Aluminum-silicon alloys are the most important and widely used materials to cast components with complex shapes, due to their excellent castability and good combination of mechanical properties and lightness (Ref 2). As customers demand larger diameter wheels and low-profile tires, the additional thickness of the rim compensates for any weakness of mechanical properties due to casting defects. However, this necessitates the design of heavier wheels which eliminates the advantage of weight saving. Engineers must further develop new forming techniques which enable the optimized manufacture of light wheels.

Yin-Chun Cheng and **Shih-Yuan Hsu**, Department of Mechanical Engineering, National Central University, No. 300, Jhongda Rd., Jhongli City, Taoyuan County 32001, Taiwan, ROC; **Chih-Kuang Lin** and **Sheng-Long Lee**, Department of Mechanical Engineering, National Central University, No. 300, Jhongda Rd., Jhongli City, Taoyuan County 32001, Taiwan, ROC; and Institute of Materials Science and Engineering, National Central University, Chungli, Taiwan, ROC; and **An-Hung Tan,** Department of Mechanical Engineering Ching-Yun University, No. 229, Jianxing Rd., Zhongli City, Taoyuan County 32097, Taiwan, ROC. Contact e-mails: hz2407@yahoo.com.tw, t330014@cc.ncu.edu.tw, ahtan@cyu.edu.tw, sico4444@yahoo.com.tw, and shenglon@cc.ncu.edu.tw.

Spinning deformation processing (SDP) refers to a group of forming processes for the production of hollow and axially symmetric metal components in small to medium batches. This process involves clamping the preform against a mandrel on a spinning lathe and plastic deformation of the material along the profile of the mandrel achieved by the set of the roller (Ref 3). A component with the thickness of 2.7 mm that has been manufactured by SDP exhibits the same mechanical strength to the one that has been cast with the thickness of 4.5 mm (Ref 4). The previous study reported that SDP improved the corrosion resistance of A356 alloy (Ref 5). This makes SDP a good potential technique for the manufacture of wheels for automobiles. As well, engineers can expect to save material costs with this process. Many studies have focused on the optimization of facilities and parameters, and how to construct the mechanics of SDP (Ref 3, 6), but there is still little understanding on the SDP strengthening mechanism for A356 alloy. To remedy this shortcoming this study examines a novel application of this process for A356 alloy. The A356 alloy preform is shaped into a wheel profile by SDP. The authors further study the strengthening mechanism of SDP for these types of alloy. The findings will provide a certain basis for wheel designers.

2. Experimental Procedure

The preform for SDP was prepared by melting commercially available strontium (Sr)-modified A356 alloy. The melt was poured into a permanent mold and air cooled. The composition of the A356 alloy as measured by a glow discharge spectrometer was Al-7.1Si-0.3Mg-0.12Fe-0.11Ti-0.01Sr wt.%. A three-roller SDP was performed to shape the preform against the mandrel. The preform attached to the mandrel was rotated at a speed of 200 rpm and heated to a temperature of 350 °C. Three rollers, A, B, and C, with tip radii of 10, 10, and 5 mm, respectively, swept across the spinning preform through multiple passes in the sequence A-B-C. The preform was designed to be a symmetrical casting with a solid line pattern, as shown in Fig. 1. The deformation after SDP, as indicated by

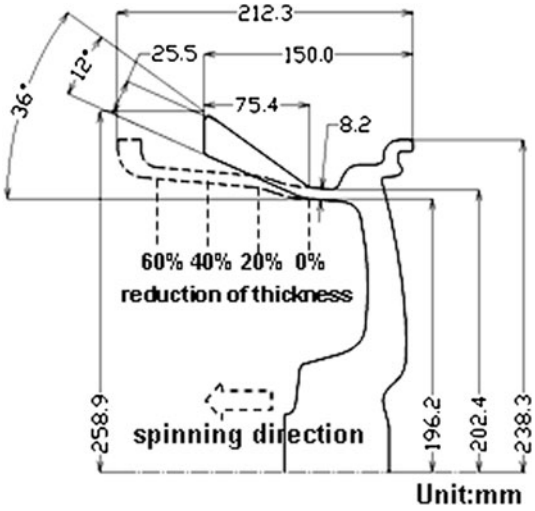

Fig. 1 Schematic illustration of the workpiece for the SDP: the preform is indicated by the solid line; the dashed lines indicate the profile of the spinning deformed portion

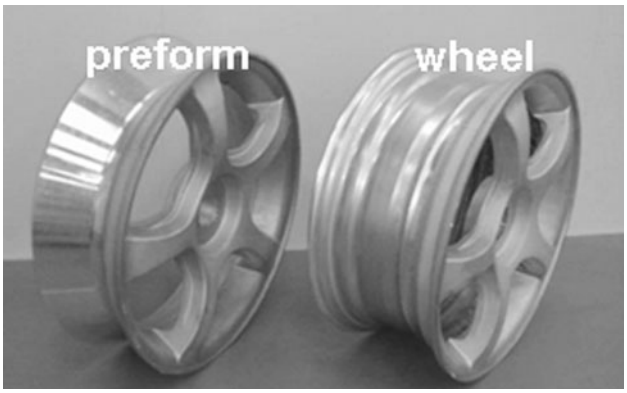

Fig. 2 Photograph of the preform and the wheel after spinning

the dashed line, reduced the thickness from 0 to 60%. Figure 2 revealed the preform and the wheel after SDP.

The microstructure on the surface perpendicular to the tangential direction of the spinning deformed sample was observed by optical microscopy (OM). The IMAQ 6.0 software was used to quantify the average area and aspect ratio of the eutectic silicon phase. The measurements for eutectic silicon particles were carried out over 20 fields (1 field = 60,902 μm^2) according previous studies (Ref 7, 8). The microstructural characteristics from those measurements are consistent. The scanning electrical microscopy (SEM JEOL-6360) was used to image the microstructure of the alloy. The Al-matrix was removed by etching with a mixture of 15 mL of HCl, 10 mL of HF, and 90 mL of distilled water. The hardness was measured using a Rockwell tester with an F scale indenter in the 60 kg load configuration. The plates of 2 mm thickness for hardness test were cut from the rim portion by wire electrical discharge machining (WEDM). The indentations were made on the surface perpendicular to the radical direction and at intervals of 5 mm. The hardness of top (near roller), central, and bottom (near mandrel) area was investigated at various reductions of thickness. The spinning deformed sample was T6 heat treated as a solid solution at 540 °C for 6 h and artificially aged at 155 °C for 3 h. Specimens with a gauge length of 13 mm and 6×2 (mm^2) in cross-sectional dimensions were cut for tensile strength testing along the axial direction by WEDM. The tensile tests were performed at room temperature using the Instron machine with a fixed cross head speed of 5×10^{-3} mm/s. The fractured surface of the tensile specimen was observed by SEM.

3. Results and Discussion

3.1 Microstructure

The local microstructure characteristics of the spinning deformed sample near the surface in contact with the roller are shown in Fig. 3. The α-Al phases apparently become elongated with increasing reduction in thickness (5-9%) in the axial direction. The interdendritic regions are also somewhat distributed. These are microstructure characteristics typically caused by SDP for Al-7Si alloy. Plastic strain induced by the roller produces shear and bending deformation during the first pass of processing, which forces the material to become fully in contact with the mandrel. The workpiece experiences increased plastic strain in subsequent SDP passes, which is dependent upon the reduction in thickness. Images of the microstructure observed at 0% (as-cast) and 60% reduction in thickness are shown in Fig. 4. A typical Al-Si hypoeutectic cast structure consisting of α-Al phase with an interdendritic region of fibrous eutectic silicon phase is shown in Fig. 4(a). In addition, the casting defects as shrinkages and gas porosities were also found in the castings. The average area of the fibrous eutectic silicon particle was 3.8 ± 0.6 μm^2 and the aspect ratio was 1.6 ± 0.3, showing a well-modified structure with Sr (Ref 8). The effect of SDP on the microstructure is illustrated in Fig. 4(b). It can be seen that the SDP elongates the α-Al phase, eliminates the casting defects and re-arranges the eutectic region. The density of casting is increased from 2.67 to 2.68 g/cm^3 due to elimination of casting defects via SDP (60% reduction) (Ref 5). The average area and the aspect ratio of the eutectic silicon particle after SDP were 3.2 ± 0.4 μm^2 and 1.5 ± 0.3, respectively. This represents a reduction of 16% ($3.8 \rightarrow 3.2$ μm^2) in the average area and 8% ($1.6 \rightarrow 1.5$) in the aspect ratio of the eutectic silicon particle. The principal force from the radial and axial directions in the SDP elongates the casting structure. Thus the fine eutectic silicon particles are distributed throughout the Al-matrix and casting defects are reduced. After the T6 treatment is applied, the eutectic silicon particle becomes spherical and significantly coarsens in comparison with that of the as-received A356 alloy. The average area of the eutectic silicon particle decreased from 8.1 ± 3.1 μm^2 of the casting-T6 A356 alloy (Fig. 4c) to 7.5 ± 2.2 μm^2 for the spinning-T6 A356 alloy (Fig. 4d). The average aspect ratio of the eutectic silicon particle also decreased from 1.5 ± 0.5 for the casting-T6 alloy to 1.4 ± 0.3 for the spinning-T6 A356 alloy. After deep etching of the Al-matrix, the eutectic silicon phase of the casting-T6 A356 alloy takes on a coral shape as shown in Fig. 5(a). The eutectic silicon phase of the spinning-T6 A356 alloy displays a finer particle shape, as seen in Fig. 5(b). The minor difference from the measurement of the eutectic silicon particle between the casting-T6 and the spinning-T6 A356 alloy stays in the range of standard deviation, which is probably just a local characterization of the coral-like eutectic silicon phase in the two-dimensional observations. Nevertheless, the break-up of the eutectic silicon phase is clearly a result of the severe

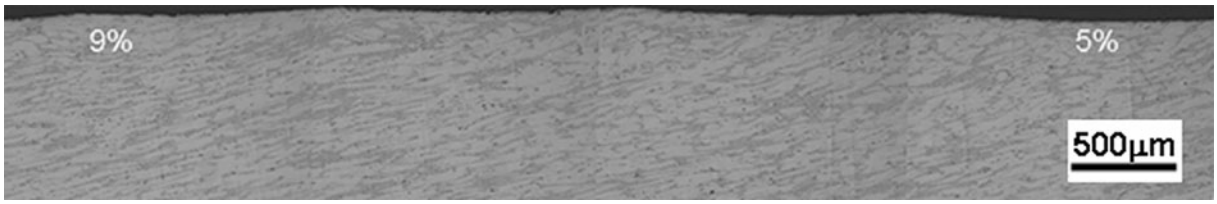

Fig. 3 Local microstructure characteristic of the SDP A356 alloy (5-9% reduction of thickness) near the surface in contact with the roller

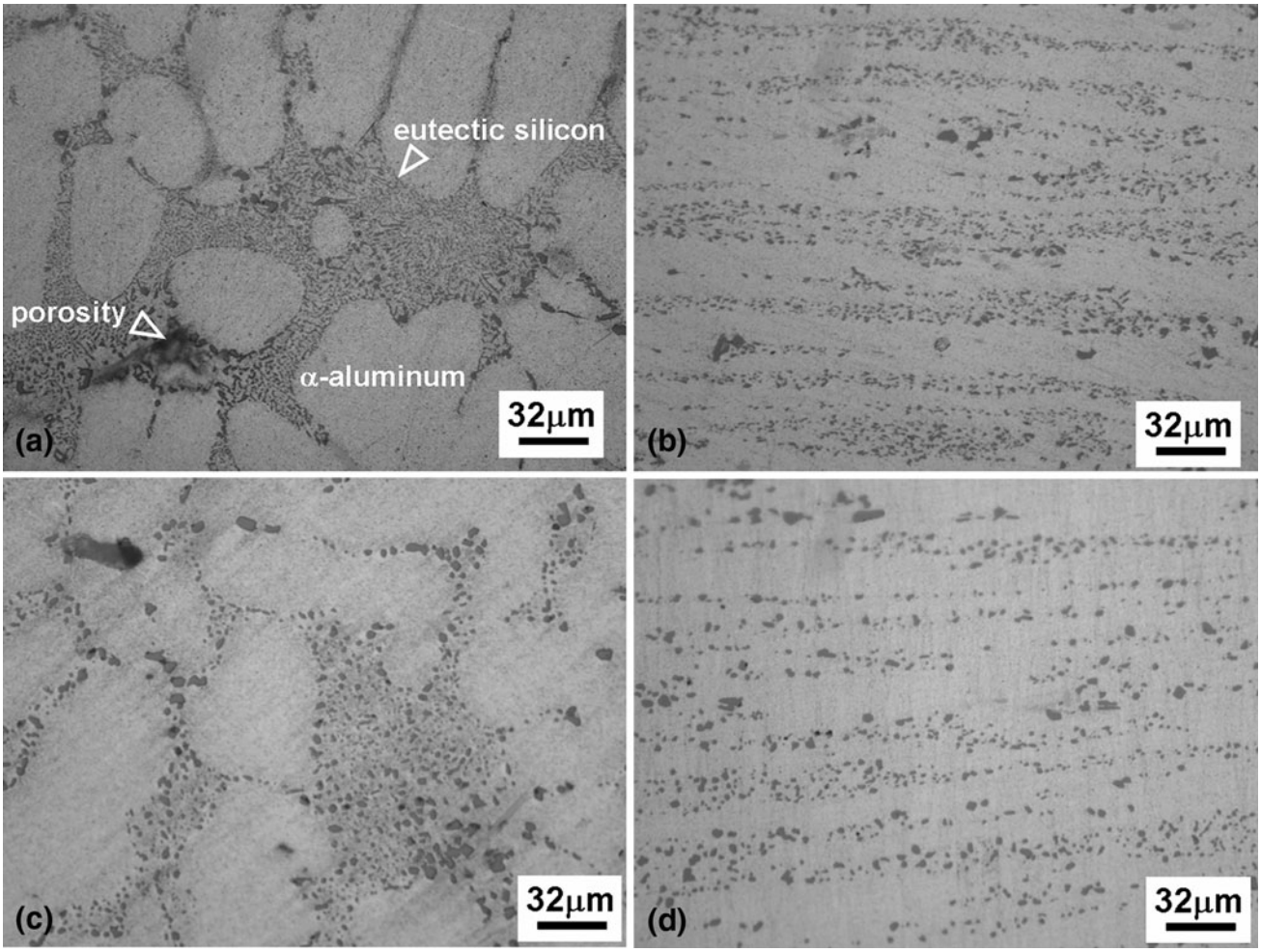

Fig. 4 OM images for A356 alloy: (a) 0%, (b) 60% reduction of thickness as-deformed and (c) 0%, (d) 60% reduction of thickness after T6 heat treatment

plastic deformation caused by the addition of the SDP to the A356 alloy. Figure 5 attests that the minor difference on the conventional polished surface is reliable. The effect of reducing the aspect ratio of the eutectic silicon phase due to SDP improves microstructure over that of using Sr to modify the melt prior to casting.

3.2 Mechanical Properties

The hardness of the spinning deformed sample was investigated after various reductions in thickness (Fig. 6). The Al-matrix is generally softer than eutectic silicon phase in hypoeutectic Al-Si alloys. The indentations for the different phases cause variation in hardness measurement. The highest value for standard deviation of hardness was observed for the 0% reduction of thickness. The standard deviation then decreased with increasing reduction in thickness due to the uniformity of the microstructure. The average hardness decreases with increasing reduction of thickness due to refinement of the eutectic silicon phase caused by plastic strain. The alloy hardness is a property for the resistance to local plastic deformation. When the indenter is forced into the material surface with a fixed load and speed, the softer material reveals the larger and deeper indentation, which means the lower hardness value. As compared to the indentation of the Al-7Si alloy and commercial pure Al alloy, the eutectic Si particles should be the predominant factor to resist the local plastic deformation. The interdendritic coral-like eutectic Si particles

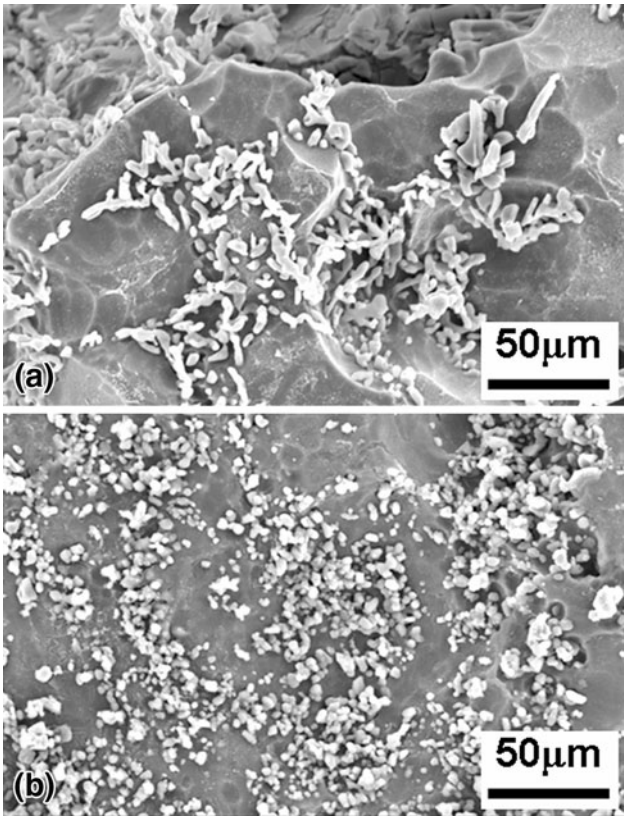

Fig. 5 SEM images for deep etching A356 alloy (a) 0%, (b) 60% after T6 heat treatment

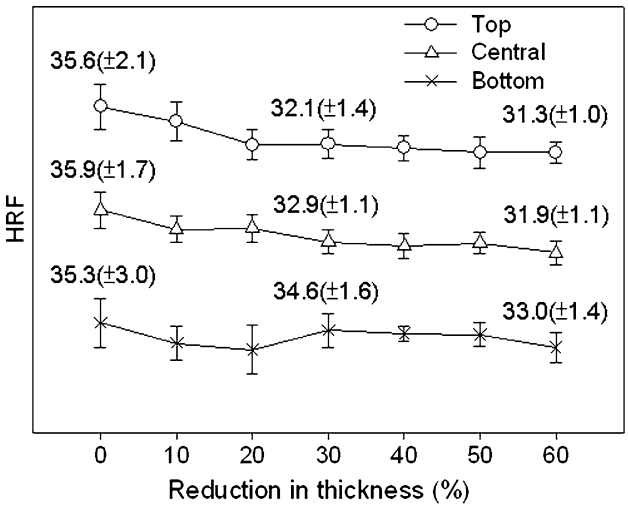

Fig. 6 Distribution of hardness for as-received SDP A356 alloy at various reductions of thickness

having rigid nature significantly increases the hardness of Al-7Si alloy in contrast to commercial pure Al alloy. However, the particle-like eutectic Si particles are distributed throughout the Al-matrix by SDP and provide less resistance to plastic deformation in contrast to the coral-like one (0% reduction), thus reveal the somewhat lower hardness as compared to the alloy absence of SDP. The minor decrease of hardness due to the modification of eutectic Si particles had been reported in previous works which correspond to present data (Ref 9, 10).

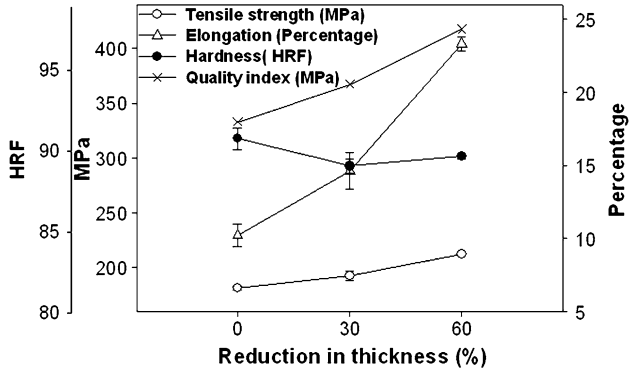

Fig. 7 Mechanical properties (i.e., hardness, tensile strength, elongation, and quality index) of an SDP A356 alloy at various reductions of thickness after T6 treatment

The decreased percentage of average hardness and standard deviation was higher in the top area than in the bottom area due to different contact sequences of roller and mandrel. During the first pass there is minimal contact between the workpiece and the mandrel, the plastic strain is close to zero at bottom area and increases at the top area. During the second and the third pass the workpiece is in full contact with the mandrel, plastic strain is imparted to the bottom area initially and accumulated to the top area. Thus the local plastic strain increased more rapidly near the roller (top area) than near the mandrel (bottom area) as the reduction in thickness increased (Ref 11). This resulted in a uniformity of the microstructure and even hardness at 60% reduction in thickness.

The A356 alloy is a kind of heat treatable alloy which can be age-hardened given proper heat treatment. The mechanical properties are greatly improved by precipitation of the Mg_2Si phase (Ref 12). The mechanical properties (i.e., hardness, tensile strength, elongation, and quality index) of spinning deformed sample in the T6 heat treatment condition were examined at various reductions of thickness (Fig. 7). The hardness of the spinning deformed sample was increased by the T6 heat treatment, but decreased somewhat with increasing reduction in thickness due to refinement of the eutectic silicon phase. When the SDPed (60% reduction in thickness) A356 alloy as-received in contrast to A356 alloy as-cast (0% reduction in thickness), the SDP changes the distribution of the interdendritic eutectic region and does not increase the alloy hardness. The microstructural characteristic is recognizable between spinning-T6 and casting-T6 even if the T6 heat treatment is processed. The hardness is increased by T6 heat treatment and retains similar value between spinning-T6 and casting-T6. This demonstrates that the SDP produces microstructural characteristic and is helpless for improvement of hardness and development of precipitation. In the previous studies, the most effective and commonly used method for eutectic modification has been the addition of chemical modifier (Ref 8, 13). The modification of the alloy structure through the addition of Sr leads to the development of a fibrous eutectic structure, as shown in Fig. 4(a). The geometrical change (from acicular to fibrous eutectic Si) leads to the disappearance of stress raisers and improvement in the tensile properties. However, the formation of porosity which accompanies the addition of Sr may affect the mechanical properties to some extent. The SDP enhances the microstructure of the A356 alloy more than that modified by Sr. The characteristics

of the microstructure have a significant influence on the material fracturing. Table 1 clearly shows that the trend of the improvement for the SDPed A356 alloy is identical when the tensile properties measured in as-received or T6 heat treatment condition. The tensile strength and elongation are enhanced with increasing reduction in thickness, as shown in Fig. 7. The presence of the fine eutectic silicon phase with its small aspect ratio retards crack nucleation due to a reduction of the stress concentration effect on the particles. This diminishes the crack nucleation, and can contribute to a decrease in the crack growth rates (Ref 14). Thus, the stress or strain required to fracture a SDP sample is significantly higher than that required to fracture a casting. The trend of increasing tensile strength being associated with increased ductility is typical of plastic deformed A356 alloy (Ref 10, 15). When evaluating the tensile properties they are usually considered separately when the effect of one or more parameters must be taken into account. The quality index proposed by Drouzy et al. (Ref 16) simplifies the influence of many variables on tensile properties and facilitates the interpretation of data regarding tensile properties. These are directly related to the physical properties of the alloy and also very independently of each other. Drouzy defined the quality index as follows: Q = UTS (MPa) + 150 log (%E). The quality index for the SDPed sample after the T6 heat treatment is displayed in

Table 1 Average area of eutectic silicon particle and tensile properties of A356 alloy as various reductions of thickness

	As-received				T6-treated			
	Average area of Si particle, μm^2	Tensile strength, MPa	Elongation, %	Quality index, MPa	Average area of Si particle, μm^2	Tensile strength, MPa	Elongation, %	Quality index, MPa
0% Reduction	3.8 (±0.6)	87.3 (±5.3)	12.1 (±2.5)	249.7	8.1 (±3.1)	181.4 (±3.7)	10.2 (±1.5)	332.7
30% Reduction	3.6 (±0.6)	100.4 (±7.1)	26.7 (±3.1)	314.4	7.7 (±2.8)	192.4 (±8.8)	14.6 (±2.5)	367.1
60% Reduction	3.2 (±0.4)	102.6 (±3.2)	31.2 (±1.5)	326.7	7.5 (±2.2)	212.3 (±3.8)	23.3 (±1.0)	417.4

Standard deviation is listed in parenthesis

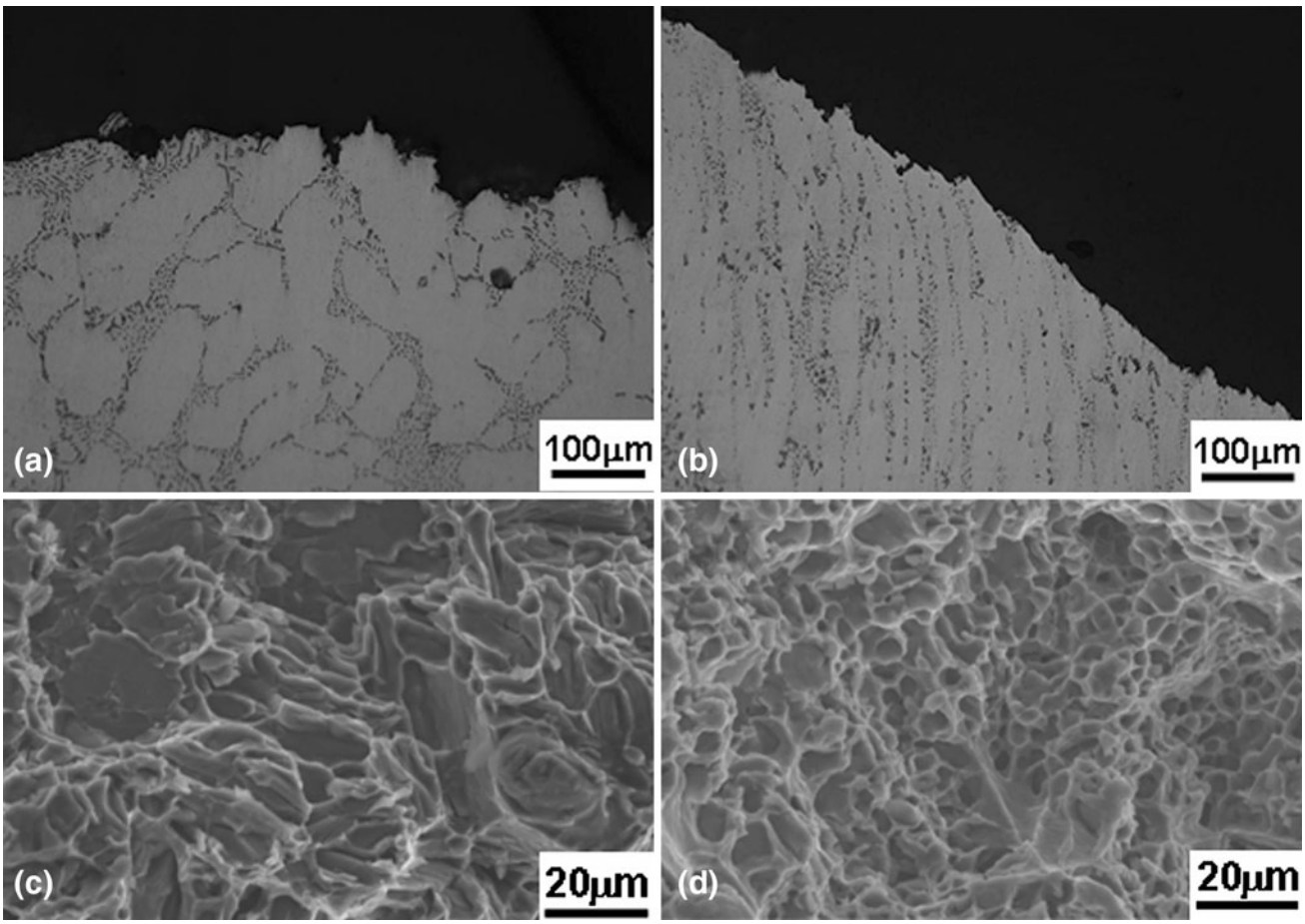

Fig. 8 Observation of the tensile fracture of SDP A356 alloy after T6 treatment: cross-sectional images observed by OM for (a) 0%, (b) 60% reductions of thickness; fractured surface observed by SEM for (c) 0%, (b) 60% reductions of thickness

Fig 7. The quality index shows the enhancement by increasing reduction of thickness. The best quality index is produced by the improvement of tensile strength and elongation due to the refined microstructure.

Observations of tensile fractures are revealed in Fig. 8. The propagation path of the final crack explains the difference in elongation due to the reduction in thickness. In the cast sample (with 0% reduction of thickness), the path propagates through the eutectic region, as observed in Fig. 8(a). After nucleation of the crack in the eutectic region, it propagates through the regions offering less resistance. However, the crack becomes smooth when it passes through both eutectic and α-Al regions (Fig. 8b). In this case, the SDP elongates the α-Al phase and distributes the fine eutectic silicon phase throughout the Al-matrix. Therefore, the crack which has nucleated in the eutectic region is forced to propagate through the α-Al phase. The elongated α-Al phase is more ductile than the eutectic region. It acts as a barrier to crack coalescence and increases ductility. As for the casting defects, they are harmful to mechanical properties. However, the quantity of defects is lower than that of eutectic Si particles in the casting. Many researchers consequently indicated that the fracture of A356 alloy is predominantly due to eutectic Si particle (Ref 8, 10, 14). When the SDP is performed on A356 alloy, the elongated structure results the elimination or reduction of defects. The improvement of mechanical properties comes from the re-arrangement of eutectic region and the elimination (or reduction) of defects. Nevertheless, the effect of re-arrangement of eutectic region on the mechanical properties is significant in contrast to that of eliminating (or reducing) defects. The as-cast sample (0% reduction of thickness) showed several cleavages of the broken eutectic silicon phase and some uneven size dimples on the fractured surface, as illustrated in Fig. 8(c). The fracturing mode of Sr-modified A356alloy is generally ductile (Ref 8). Nevertheless, the surface fracturing changed to finer dimple ruptures (5-8 μm) in SDP 60% reduction of thickness sample (Fig. 8d). This exposes the ease of crack nucleation and propagation on the fractured surface of the Sr-modified A356 alloy in comparison to spinning-deformed A356 alloy and further demonstrates the improvement of ductility produced by SDP.

4. Conclusion

An A356 casting preform was shaped into a wheel shape by SDP in this study. The SDP reduced casting defects, refined and re-arranged the eutectic silicon phase as well as facilitated microstructural uniformity. These microstructural characteristics had significant influence on the material fracturing. Thus, the tensile strength was increased by SDP. Elongation was also increased due to differences in the distribution of the eutectic region. Cracks nucleated at the Al/Si interface and propagated through the eutectic region in the cast structure. The SDP distributed the fine eutectic silicon throughout the Al-matrix, which forced the cracks to propagate through the ductile α-Al phase. The ductility increased accordingly. The improved ductility resulted increase in tensile strength as well. The surface fracturing revealed overall fine dimple ruptures when the sample produced by SDP reached a 60% reduction of thickness. The improvement on tensile strength and elongation produced the best quality index for A356 alloy.

Acknowledgments

The authors would like to thank the National Science Council of the Republic of China, Taiwan for financially supporting this research under Contract No. NSC99-2622-E-008-007-CC3.

References

1. D. Carney, Wheel Design and Engineering, *Autom. Eng. Int.*, 2001, **109**, p 54–59
2. M. Merlin, G. Timelli, F. Bonollo, and G.L. Garagnani, Impact Behaviour of A356 Alloy for Low-pressure Die Casting Automotive Wheels, *J. Mater. Process. Technol.*, 2009, **209**, p 1060–1073
3. C.C. Wong, T.A. Dean, and J. Lin, A Review of Spinning, Shear Forming and Flow Forming Processes, *Int. J. Mach. Tools Manuf.*, 2003, **43**, p 1419–1435
4. D. Polit, Metal Spinning in the Automotive Industry, *Sheet Met. Ind.*, 1995, **72**, p 31–32
5. Y.C. Cheng, C.K. Lin, A.H. Tan, J.C. Lin, and S.L. Lee, Effect of Spinning Deformation Processing on the Wear and Corrosion Properties of Al-7Si-0.3Mg Alloys, *Mater. Manuf. Process.*, 2010, **25**, p 689–695
6. O. Music, J.M. Allwood, and K. Kawai, A Review of the Mechanics of Metal Spinning, *J. Mater. Process. Technol.*, 2010, **210**, p 3–23
7. A.M.A. Mohamed, A.M. Samuel, F.H. Samuel, and H.W. Doty, Influence of Additives on the Microstructure and Tensile Properties of Near-Eutectic Al-10.8%Si Cast Alloy, *Mater. Des.*, 2009, **30**, p 3943–3957
8. Y.C. Tsai, C.Y. Chou, S.L. Lee, C.K. Lin, J.C. Lin, and S.W. Lim, Effect of Trace La Addition on the Microstructures and Mechanical Properties of A356 (Al–7Si–0.35Mg) Aluminum Alloys, *J. Alloys Compd.*, 2009, **487**, p 157–162
9. Z. Ma, E. Samuel, A.M.A. Mohamed, A.M. Samuel, F.H. Samuel, and H.W. Doty, Influence of Aging Treatments and Alloying Additives on the Hardness of Al-11Si-2.5Cu-Mg Alloys, *Mater. Des.*, 2010, **31**, p 3791–3803
10. C.Y. Chou, K.W. Wang, S.L. Lee, and T.S. Yang, Modifying Al–7Si–0.35Mg Alloys Using Equal Channel Angular Extrusion, *Mater. Lett.*, 2008, **62**, p 2469–2472
11. M.J. Roy, R.J. Klassen, and J.T. Wood, Evolution of Plastic Strain During a Flow Forming Process, *J. Mater. Process. Technol.*, 2009, **209**, p 1018–1025
12. D.L. Zhang and L. Zheng, The Quench Sensitivity of Cast Al-7 Wt Pct Si-0.4 Wt Pct Mg Alloy, *Metall. Mater. Trans. A*, 1996, **27A**, p 3983–3991
13. C.Y. Yang, S.L. Lee, C.K. Lee, and J.C. Lin, Effect of Sr and Sb Modifiers on the Sliding Wear of A357 Alloy Under Varying Pressure and Speed Conditions, *Wear*, 2006, **261**, p 1348–1358
14. F.T. Lee, J.F. Major, and F.H. Samuel, Effect of Silicon Particles on the Fatigue Crack Growth Characteristics of Al-12 wt pct Si-0.35 wt pct Mg-(0 to 0.02) wt pct Sr Casting Alloys, *Metall. Mater. Trans. A*, 1995, **26**, p 1553–1570
15. M.L. Santella, T. Engstron, D. Storjohann, and T.Y. Pan, Effect of Friction Stir Processing on Mechanical Properties of the Cast Aluminum Alloys A319 and A356, *Scripta Mater.*, 2005, **53**, p 201–206
16. M. Drouzy, S. Jacob, and M. Richard, Le Diagramme Charge de Rupture des Alliages d'aluminium, *Foundries*, 1976, **355**, p 139–147